*International Journal of Thermophysics, Vol. 23, No. 5, September 2002 (© 2002)*

# Development of a Special Multi-Wavelength Pyrometer for Temperature Distribution Measurements in Rocket Engines[1]

**X. G. Sun,[2] J. M. Dai,[2, 3] D. C. Cong,[2] and P. Coppa[4]**

Previously a fast multi-wavelength pyrometer was developed in a collaboration between the Harbin Institute of Technology of China and Rome University of Italy. The main features of the instrument include the use of a dispersing prism and a photodiode array to cover the entire spectral band. Following this experience, a new type of six-target eight-wavelength pyrometer for solid propellant rocket engine plume temperature distribution measurements has been developed. The instrument can record the radiation fluxes of eight wavelengths for six different uniformly distributed points on the target surface, which are well defined by holes on a field stop. The fast pyrometer with a specially designed synchronous data acquisition system can assure that the recorded thermal radiation fluxes of different spectral regions are at the same time and the same true temperature, even with dramatically changed targets.

**KEY WORDS:** fast data acquisition; multi-target multi-wavelength pyrometer; plume temperature; solid propellant rocket engine.

## 1. INTRODUCTION

Multi-wavelength techniques [1–3], which can simultaneously perform true temperature and emissivity measurements without using any auxiliary means, have been the focus of important research in the field of radiation thermometry. The plume temperature of a solid propellant rocket engine is a fundamental parameter in denoting combustion status. It is necessary to

[1] Paper presented at the Sixth International Workshop on Subsecond Thermophysics, September 26–28, 2001, Leoben, Austria.

[2] Department of Automation Measurement and Control Engineering, Harbin Institute of Technology, P.O. Box 308, Harbin 150001, People's Republic of China.

[3] To whom correspondence should be addressed. E-mail: djm@hope.hit.edu.cn

[4] Department of Mechanical Engineering, University of Rome 'Tor Vergata,' Rome, Italy.



0195-928X/02/0900-1293/0 © 2002 Plenum Publishing Corporation

measure the temperature along both the axis and the radius of the engine. Existing radiation thermometers can only measure a single target point. Although multi-target point measurements can be realized by using scanning equipment or using several multi-wavelength thermometers, it is not easy to record the thermal radiation fluxes of different spectral regions at the same time with dramatically changed targets such as the plume of a solid propellant rocket engine. Al was added into the solid propellant to improve the charateristics of the propellant. So among the plume of a solid propellant rocket engine, there were many $Al_2O_3$ particles.

In order to measure the plume temperature distribution of a solid propellant rocket engine, a new type of six-target eight-wavelength pyrometer has been successfully developed in a collaboration between the Harbin Institute of Technology of China and Rome University of Italy. The main features of the instrument include the use of a dispersing prism and of Si-photodiodes to cover the entire spectral band 0.5 to 1.0 μm. A special field stop is used in order to simultaneously aim at six-target points (the interval distance can be adjusted). The instrument can record the radiation fluxes of eight wavelengths for six uniformly distributed points on the target surface. A specially designed S/H (Sample/Hold) circuit, with 48 sample and hold units that were triggered with a signal, measures the multi-wavelength and multi-target outputs. It can sample 48-signals in less than 10 ns time difference (which is most important for the temperature calculation).

## 2. SIX-TARGET EIGHT-WAVELENGTH PYROMETER

### 2.1. Optical System

The optical system design is the first step used to develop multi-target multi-wavelength pyrometers. The basic optical design of the new six-target eight-wavelength pyrometer is shown in Fig. 1. In order to measure the radiation fluxes of eight wavelengths for six uniformly distributed points on the target surface, it is necessary to use an off-axis optical system.

Radiation emitted by the target T is focused by the object lens L1 on a field stop (FS), which is on the focal plane of the collimating lens L2. The six holes on the FS correspond to the uniformly distributed six-target points. The parallel beam generated by the collimating lens L2 is dispersed by prism P and dark chamber lens L3 focuses the slit in its focal plane, one image for each wavelength.

The positions of the target spectral images are not on a plane but on a curved surface. Therefore, single S1336-18BK Si-photodiodes (Hamamatsu Corp., Japan), and not a photodiode array are selected as detectors. The position of a single detector can be adjusted to obtain the optimum image.

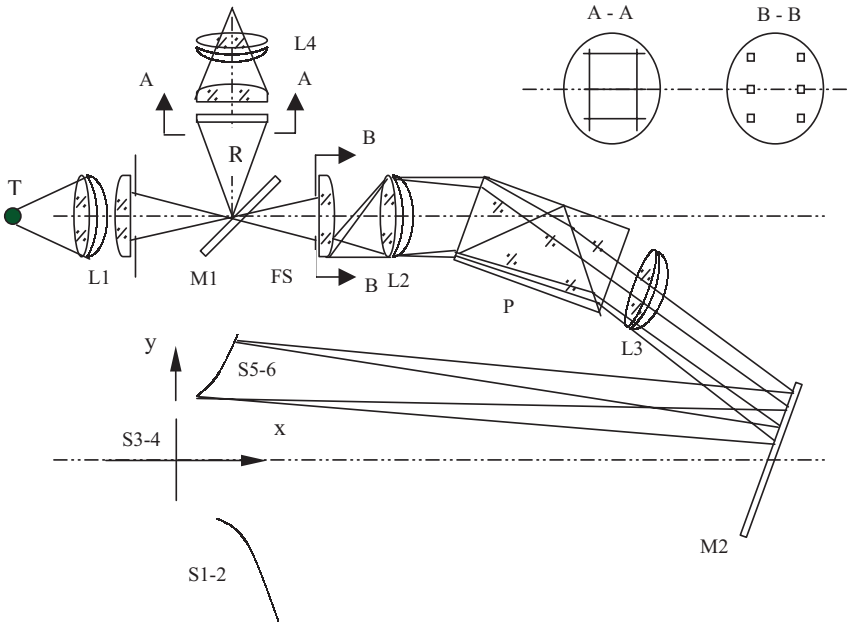


**Fig. 1.** Schematic diagram of the optical system. L1: object lens; M1: mirror; FS: field stop. L2: collimating lens; P: prism; L3: dark chamber lens. M2: mirror; L4: eyepiece; S1-2, S3-4, S5-6: detectors. R: reticle; T: target.

The radiation fluxes emitted from six targets ($4 \times 4$ mm$^2$) are precisely focused on the detectors measured at a standard distance of 6 m.

The reticle of the aiming system is at the conjugate position of the FS. The dimension of the hole on the FS is $1/40$ of the standard target dimension ($4 \times 4$ mm$^2$). The mirror M1 is at different positions when measuring or aiming. Turning the mirror M1 to an angle of 45°, adjusting the object lens, when the image of the target coincides with the point of intersection on the reticle of the aiming system, the radiation fluxes emitted from the target at a certain angle will reach the detectors through the holes on the FS. When turning the mirror M1 to the horizontal position, the measurement can start.

## 2.2. Synchronous Data Acquisition System

The six-target eight-wavelength pyrometer with the specially designed synchronous data acquisition system, can assure that the thermal radiation fluxes of different spectral regions are recorded at the same time. This is very important for temperature calculations using a multi-wavelength

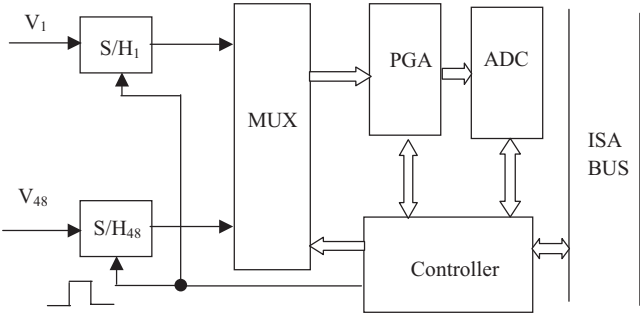


**Fig. 2.** Diagram of the synchronous data acquisition system. $V_1$: output of detector 1 (pre-amplified already); $V_{48}$: output of detector 48 (pre-amplified already); $S/H_1$: sample and hold unit 1; $S/H_{48}$: sample and hold unit 48; PGA: program control gain amplifier; ADC: analog-to-digital converter; MUX: multiplexer.

algorithm. The synchronous data acquisition system consists of sample and hold units (S/H), a multiplexer (MUX), an analog-to-digital converter (A/D), and a controller. In fact, a multichannel analog-to-digital converter card with 12 bit and 100 kHz sampling rate plugged in an industrial computer is used to acquire all 48 signals in 5 ms. The gains of the program control gain amplifier (PGA) are: $\times 1$, $\times 10$, and $\times 100$. The diagram of the synchronous data acquisition system is shown in Fig. 2.

Eight 74LS04 (Texas Corp., USA) reversers are used here. Each reverser drives six sample and hold units (S/H). The inputs of the reversers come from the same address of the 8-bit ISA data bus. Considering the differences between the eight reversers, the time differences for 48 signals are less than 10 ns.

## 3. CALIBRATION OF THE SIX-TARGET EIGHT-WAVELENGTH PYROMETER

Calibration of the six-target eight-wavelength pyrometer includes two steps: the calibration of the pyrometer wavelength function (PWF) and the calibration of the reference blackbody.

### 3.1. Calibration of the Pyrometer Wavelength Function (PWF)

In band radiation thermometry, the output of the detector can be written as

$$V(T) = G \int_{\Delta\lambda} \sigma(\lambda)\, \tau(\lambda)\, P(\lambda, T)\, d\lambda \tag{1}$$

where $P(\lambda, T)$ is the Planck function of wavelength $\lambda$ and temperature $T$, $\tau(\lambda)$ is the transmittance of all optical components, $\sigma(\lambda)$ is the detector spectral responsivity, and $\Delta\lambda$ is the pyrometer passband. $G$ is a geometrical factor involving the target area and the angle subtended by the entrance aperture of the instrument.

The ratio of signals at the unknown temperature $T$ and at a reference point $T_0$ is

$$Q = \frac{\int_{\Delta\lambda} \sigma(\lambda)\, \tau(\lambda)\, P(\lambda, T)\, d\lambda}{\int_{\Delta\lambda} \sigma(\lambda)\, \tau(\lambda)\, P(\lambda, T_0)\, d\lambda} \tag{2}$$

where $\phi(\lambda) = \sigma(\lambda)\, \tau(\lambda)$ [4] is defined as the pyrometer wavelength function (PWF); it is the product of the overall optical spectral transmittance of the pyrometer and the sensor spectral responsivity.

The mean effective wavelength $\lambda_e(T, T_0)$ is defined by the following relation

$$\lambda_e = \frac{C_2(\frac{1}{T_0} - \frac{1}{T})}{\ln Q} \tag{3}$$

where the Wien's approximation is used. $\lambda_e(T, T_0)$ changes very little with $T$, so $\lambda_e$ between a certain temperature $T$ and a reference point $T_0$ is often used as the effective wavelength of a pyrometer.

The results of the effective wavelengths of the pyrometer are shown in Table I.

The error in the calibration method results from two sources: experimental errors that directly affect the PWF, and arithmetic errors that arise in numerical integration. The error in the calibration method is less than $\pm 2$ K [5].

**Table I.** Effective Wavelengths of the Pyrometer

| Wavelength No. | Point 1 (μm) | Point 2 (μm) | Point 3 (μm) | Point 4 (μm) | Point 5 (μm) | Point 6 (μm) |
|---|---|---|---|---|---|---|
| 1 | 0.572 | 0.574 | 0.575 | 0.579 | 0.574 | 0.563 |
| 2 | 0.597 | 0.595 | 0.598 | 0.607 | 0.592 | 0.590 |
| 3 | 0.622 | 0.627 | 0.628 | 0.637 | 0.623 | 0.614 |
| 4 | 0.655 | 0.656 | 0.658 | 0.674 | 0.654 | 0.648 |
| 5 | 0.692 | 0.704 | 0.702 | 0.712 | 0.698 | 0.682 |
| 6 | 0.751 | 0.747 | 0.748 | 0.776 | 0.748 | 0.735 |
| 7 | 0.804 | 0.823 | 0.827 | 0.850 | 0.826 | 0.804 |
| 8 | 0.905 | 0.904 | 0.923 | 0.964 | 0.914 | 0.919 |

**Table II.** Outputs of the Pyrometer at the Reference Blackbody ($T = 2252$ K)

| Wavelength No. | Point 1 (mV) | Point 2 (mV) | Point 3 (mV) | Point 4 (mV) | Point 5 (mV) | Point 6 (mV) |
|---|---|---|---|---|---|---|
| 1 | 75.63 | 51.98 | 90.54 | 84.68 | 39.44 | 64.60 |
| 2 | 108.56 | 88.31 | 103.51 | 155.26 | 139.74 | 86.58 |
| 3 | 160.84 | 140.29 | 161.15 | 254.14 | 117.53 | 183.74 |
| 4 | 273.65 | 207.26 | 345.82 | 390.87 | 363.66 | 200.57 |
| 5 | 481.33 | 465.44 | 359.12 | 671.64 | 345.01 | 496.74 |
| 6 | 433.47 | 335.69 | 557.78 | 586.26 | 493.94 | 415.16 |
| 7 | 286.86 | 340.86 | 336.41 | 365.10 | 320.73 | 454.76 |
| 8 | 319.06 | 233.96 | 498.57 | 437.54 | 406.67 | 995.74 |

### 3.2. Calibration of the Reference Blackbody

The outputs of the pyrometer at the reference blackbody (the temperature is 2252 K) are shown in Table II.

The effective emissivity of the calibration blackbody source is more than 0.99. The error in the calibration source is less than $\pm 2$ K.

## 4. EVALUATION PROCEDURE

If a multi-wavelength pyrometer has $n$ channels, then the output $V_i$ at the $i$th channel can be written as

$$V_i = G_i \varepsilon(\lambda_i, T)\, C_1 \lambda_i^{-5} e^{-\frac{C_2}{\lambda_i T}} \qquad (i = 1, 2, \ldots, n) \tag{4}$$

where $\lambda_i$ is the effective wavelength of the $i$th channel (see Section 3.1), $\varepsilon(\lambda_i, T)$ is the spectral emissivity at the wavelength $\lambda_i$ and temperature $T$, $C_1$ is the first radiation constant, and $C_2$ is the second radiation constant.

At the reference blackbody temperature $T'$, the output $V_i'$ at the $i$th channel is

$$V_i' = G_i C_1 \lambda_i^{-5} e^{-\frac{C_2}{\lambda_i T'}} \qquad [\text{now} \quad \varepsilon(\lambda_i, T) = 1.0] \tag{5}$$

Combining Eqs. (4) and (5) leads to

$$\frac{V_i}{V_i'} = \varepsilon(\lambda_i, T)\, e^{-\frac{C_2}{\lambda_i T}} e^{\frac{C_2}{\lambda_i T'}} \tag{6}$$

where it is unnecessary to know how much $G_i$ is, because in Eq. (6) $G_i$ has been canceled out.

The relationship between emissivity and wavelength is represented as a polynomial

$$\ln \varepsilon(\lambda, T) = \sum_{i=0}^{m} a_{i+1}\lambda^i \qquad (m \leqslant n-2) \tag{7}$$

If $Y_i = \lambda_i \ln(\frac{V_i}{V_i'}) - \frac{C_2}{T'}$, $a_0 = -\frac{C_2}{T}$, $X_{1,i} = \lambda_i, \ldots, X_{m,i} = \lambda_i^m$, then introducing Eq. (7) into Eq. (6) leads to:

$$Y_i = a_0 + a_1 X_{1,i} + \cdots + a_m X_{m,i} \qquad (i = 1, 2, \ldots, n;\ m < n-2) \tag{8}$$

The calculated temperatures of target 1 based on the least squares method are shown in Fig. 3. The calculated temperatures of targets $2 \sim 6$, based on the least squares method, are similar to that of target 1 in quantity.

## 5. ERROR ANALYSIS

Experimental errors result from five contributions: errors in the calibration source, in the calibration method, in the measurement distance, in the A/D converter, and in the assumption between emissivity and wavelength.

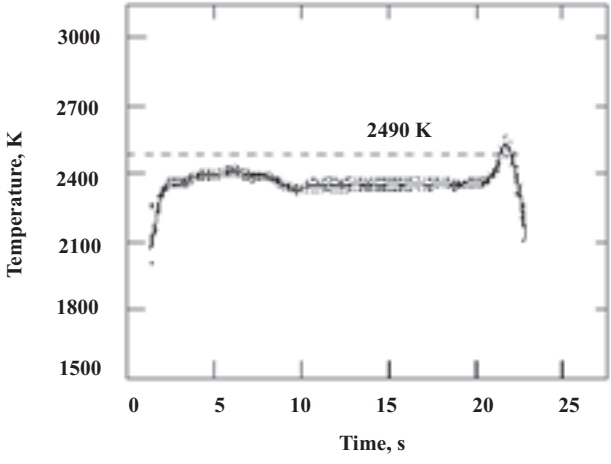


**Fig. 3.** Calculated temperatures of target 1. (——) experimental temperature; (· · · · · ·) error interval of the experimental temperature; (----) theoretical temperature from the rocket engine designer.

(a) Error in the calibration source. The effective emissivity of the calibration blackbody source is more than 0.99. The temperature precision is within $\pm 2$ K.

(b) Error in the calibration method. The error in the calibration method based on the pyrometer wavelength function is also within $\pm 2$ K [5].

(c) Error in the measurement distance. The error in the measurement distance resulting from the plume inflation is less than 1 K [6].

(d) Error in the A/D converter. The error in the A/D converter is less than 1 K because the temperature scale is 1500 to 3000 K and a 12-bit A/D converter was used.

(e) From a large number of simulated experiments [7], error resulting from the assumption between emissivity and wavelength is less than $\pm 40$ K.

The total experimental error can be written as

$$e^2 = e_1^2 + e_2^2 + e_3^2 + e_4^2 + e_5^2 \tag{9}$$

where $e$ is the total experimental error, $e_1$ is the error in the calibration source, $e_2$ is the error in the calibration method, $e_3$ is the error in the measurement distance, $e_4$ is the error in the A/D converter, and $e_5$ is the error resulting from the assumption between emissivity and wavelength.

The total experimental error of the temperature is less than $\pm 40$ K.

## 6. CONCLUSION

The pyrometer has been successfully used in some ground experiments to measure the plume temperature of solid propellant rocket engines with satisfactory experimental results. The system reliability design can meet the demands of the worksite. The temperature differences between the measurements and the theoretical calculations from the rocket engine designer were less than 100 K. The estimated error of the temperature is less than $\pm 40$ K.

## ACKNOWLEDGMENT

This work was supported in part by the No. 4 Research Institute of the Aerospace Industry Corporation of China.

## REFERENCES

1. J. L. Gardner and T. P. Jones, *J. Phys. E.* **13**:306 (1980).
2. P. B. Coates, *Metrologia* **17**:103 (1981).
3. Y. Chen, *High Temps.-High Press.* **24**:75 (1992).
4. P. Coppa, *High Temps.-High Press.* **22**:479 (1988).
5. J. M. Dai, *Acta Metrologica Sinica* **20**:53 (1999).
6. J. M. Dai, *J. Infrared Millim. Waves* **19**:62 (2000).
7. X. G. Sun, *J. Infrared Millim. Waves* **17**:221 (1998).